Published in final edited form as:
*Exp Neurol*. 2011 September ; 231(1): 160–170. doi:10.1016/j.expneurol.2011.06.004.

# An angiogenic inhibitor, cyclic RGDfV, attenuates MPTP-induced dopamine neuron toxicity

**Aditiben Patel**, **Giuseppe V Toia**, **Kalea Colletta**, **Brinda Desai Bradaric**, **Paul M Carvey**[1], and **Bill Hendey**

[1]Department of Pharmacology and Neuroscience, Rush University

## Abstract

We previously demonstrated that several dopamine (DA) neurotoxins produced punctate areas of FITC-labeled albumin (FITC-LA) leakage in the substantia nigra and striatum suggesting blood brain barrier (BBB) dysfunction. Further, this leakage was co-localized with αvβ3 integrin up-regulation, a marker for angiogenesis. This suggested that the FITC-LA leakage might have been a result of angiogenesis. To assess the possible role of angiogenesis in DA neuron loss, we treated mice with 1-methyl-4-phenyl-1,2,3,6 tetrahydropyridine (MPTP) and on the following day treated with cyRGDfV, a cyclic peptide that binds to integrin αvβ3 and prevents angiogenesis. Post-treatment for three days (b.i.d.) with cyRGDfV blocked the MPTP-induced upregulation of integrin β3 immunoreactivity (a marker for angiogenesis), leakage of FITC-LA into brain parenchyma (a marker for BBB disruption) as well as the down regulation of Zona Occludin-1 (ZO-1; a marker for tight junction integrity). In addition, cyRGDfV also completely prevented tyrosine hydroxylase immunoreactive cell loss (a marker for DA neurons) and markedly attenuated the up-regulation of activated microglia (Iba1 cell counts and morphology). These data suggest that cyRGDfV, and perhaps other anti-angiogenic drugs, are neuroprotective following acute MPTP treatment and may suggest that compensatory angiogenesis and BBB dysfunction may contribute to inflammation and DA neuron loss.

### Keywords

Blood Brain Barrier; ZO-1; neuroinflammation; microglia; Parkinson's disease; disease progression; angiogenesis

## Introduction

Parkinson's disease (PD) is the second most common neurodegenerative disorder after Alzheimer's disease (AD) and the most common movement disorder. Clinical symptoms are associated with a prominent degeneration of dopamine (DA) neurons in the ventral tier of the substantia nigra pars compacta (SNpc), and DA neuron terminal loss in the striatum (Antonini et al., 2002; Damier et al., 1999). Its pathogenesis is associated with a cascade of neuroinflammatory events including oxidative stress (Pearce et al., 1997), impaired



Corresponding Author: Bill Hendey: 1735 West Harrison St. (Suite 412), Rush University, Chicago, IL 60612, 312-563-2563, Bill_Hendey@rush.edu.

mitochondrial function (Zhu and Chu, 2010) accumulation of reactive oxygen species (ROS) (Fato et al., 2008), glutamate excitotoxicity (Caudle and Zhang, 2009), protein misfolding (Cuervo et al., 2010), and accumulation of α-synuclein protein due to ubiquitin-proteosomal system dysfunction (Hindle, 2010). Although neuroinflammation is clearly associated with the degenerative process, the mechanism(s) that underlie the progressive phase of PD (i.e., the inexorable progressive loss of DA neurons that occurs after the initiation of disease) remains unknown.

One mechanism that could contribute to progressive DA neuron loss includes dysfunction of the blood brain barrier (BBB; (Carvey et al., 2009) and entry into brain of peripheral inflammatory factors and immune cells. A series of studies from our laboratory (Carvey et al., 2005; Zhao et al., 2007) as well as others (Chen et al., 2008; Chung et al., 2010b) demonstrated that several DA neurotoxins produce BBB dysfunction potentially facilitating entry of peripheral elements into brain parenchyma, which could mediate a progressive neurodegeneration (Carvey et al., 2009). These toxins, including 1-methyl-4-phenyl-1,2,3,6 tetrahydropyridine (MPTP), 6-hydroxydopamine (6-OHDA), rotenone, prenatal lipopolysaccharide (LPS), and paraquat, produced punctate areas of leakage restricted to areas associated with DA neurodegeneration (Carvey et al., 2009). Interestingly, we also showed that 6-OHDA-induced BBB disruption was associated with a marked increase in integrin αvβ3 expression (an angiogenic marker) that was co-localized with the punctate areas of leakage suggesting an association between BBB disruption and angiogenesis (Carvey et al., 2005). Since angiogenesis is a compensatory response to injury or hypoxia (Marti, 2005) and newly formed angiogenic vessels are leaky (Brown et al., 1997), it is possible that the punctate areas of leakage we and others have seen in animal models of PD reflect, in part, compensatory angiogenesis. This dysfunction in barrier integrity could facilitate the entry of peripheral factors into brain (Barcia et al., 2004) thereby potentiating the degenerative process contributing to disease progression.

Expression of integrin αvβ3 is dramatically increased on vessels throughout the angiogenic process (Ginsberg et al., 2005; Hynes and Zhao, 2000; Somanath et al., 2009), but is virtually absent on patent vasculature (Brooks et al., 1994b). Since it is well established that PD is associated with a robust innate immune response (Lee et al., 2009) and both activated microglia and astroglia release a number of inflammatory cytokines that have proangiogenic activity including, TNFα, and vascular endothelial growth factor (VEGF), (Szekanecz et al., 2009), angiogenesis could be a normal response to the Parkinson's degenerative process. Indeed, VEGF, a well known pro-angiogenic factor, is elevated in both PD patients and animal models (Barcia et al., 2005; Barcia et al., 2004; Wada et al., 2006; Yasuda et al., 2007). In addition, several studies have linked alterations in vascularity with PD (Barcia et al., 2005; Faucheux et al., 1999). If compensatory angiogenesis and its associated BBB dysfunction occurs as part of the DA neurodegenerative process, then preventing angiogenesis following DA neurodegeneration may provide insight into the effect, if any, angiogenesis has on DA neuron loss. We used an anti-angiogenic cyclic RGD peptide, to assess this possibility.

The RGD (arginine-glycine-aspartic acid) sequence is found on a variety extracellular matrix molecules including fibronectin, vitronectin, osteopontin, collagens, thrombospondin, fibrinogen, and von Willebrand factor and is recognized by a variety of integrin receptors that mediate cell-substrate attachment (Ruoslahti and Pierschbacher, 1986). Not surprisingly, RGD containing peptides inhibit the binding of a variety of integrin receptors. However, cyclic forms of the RGD peptides were found to restrict their conformation and afford greater receptor specificity (Aumailley et al., 1991). cyRGDfV was identified as binding the αvβ3 vitronectin receptor (Kawaguchi et al., 2001) and consequently reduced vitronectin binding (Aumailley et al., 1991). Likewise, cyRGDfV reduced αvβ3 mediated

cell adhesion (Aumailley et al., 1991; Kawaguchi et al., 2001) and induced endothelial cell (EC) apoptosis while inhibiting angiogenesis (Brooks et al., 1994a; Brooks et al., 1994b; Maubant et al., 2006). To assess the possible role of angiogenesis in the DA degenerative process, we administered cyRGDfV on the day following MPTP treatment in mice and assessed its effects on integrin β3 expression, vascularity, BBB disruption, tight junction integrity, DA neuron loss, and microglial activation. The results were surprisingly robust suggesting that angiogenesis and its consequences may play an important role in MPTP-induced neurodegeneration.

## Materials and Methods

### Experimental Animals

A total of 41 male 8 week old mice (C57BL/6; Jackson Laboratory; Bar Harbor, ME) weighing 22-25 g at the start of study, were used. The animals were housed in groups of four or five in environmentally regulated quarters (lights on at 06.00-18.00h). All mice were acclimated to the animal facility for at least 2 weeks prior to the start of the study. One day prior to MPTP treatment, the mice were moved to a controlled, ventilated room and housed in ventilation chambers until sacrificed. Mice were allowed free access to food and water for the duration of the study. The protocols used in this study were approved by the Rush University Medical Center, Institutional Animal Care and Utilization Committee (IACUC) and were compliant with all regulations at the institutional, state and federal levels. MPTP-HCl (Sigma, St. Louis, MO) handling and safety measures followed methods described by Przedborski et al. (Przedborski et al., 2001). As with all of our studies, only animals that were overtly healthy without apparent distress and of normal appearance and weight were processed further. In this study, none of the animals were lost during the course of the study.

### Study design

MPTP-HCl (10 mg/kg, freebase) was injected (i.p) four times at 1-h intervals for a total of 40 mg/kg over a 4 hour period. MPTP was dissolved in 0.9% saline on the day of administration. Saline treated mice followed the same injection protocol. cyRGDfV (Cyclo [Arg-Gly-Asp-D-Phe-Val], Enzo Life Sciences) was administered at 100μg/50μl i.p., two times per day, 8-h apart, dissolved in phosphate buffered saline (Cellgro) for 3 consecutive days, starting on the day following the first MPTP injection with the last dose administered 12-h prior to sacrifice. Control mice received cyRADfV (Cyclo [Arg-Ala-Asp-D-Phe-Val], Enzo Life Sciences), an inactive peptide molecularly similar to cyRGDfV (Brooks et al., 1994b). One amino acid substitution in cyRADfV reduces its ability to bind integrin αvβ3 and abolishes its actions as an anti-angiogenic (Brooks et al., 1994b).

Mice (n=25) were randomly divided into five groups designated as follows: Sal/Sal= saline injections given in place of MPTP and cyRGDfV (n=5); MPTP/Sal (n=5); MPTP/cyRGDfV (n=5); MPTP/cyRADfV (n=5); and Sal/cyRGDfV (n=5). The dependent measures in this study were integrin β3 immunohistochemistry (IHC), FITC-labeled albumin (FITC-LA) leakage, and zona occludin (ZO-1) immunoreactivity (ir) to assess BBB and tight junction integrity, respectively. In addition, tyrosine hydroxylase (TH), ionized calcium binding adaptor molecule (Iba1) and Nissl IHC were done to detect TH positive DA cells, neuroinflammation, and the overall cell population, respectively, in the SN. An additional cohort of 16 mice was divided into four groups: Sal/Sal (n=4); MPTP/Sal (n=4); MPTP/cyRGDfV (n=4); and MPTP/cyRADfV (n=4) and used to perform double label immunofluorescence experiments. FITC-LA was co-localized with integrin β3 (Texas Red) and FITC-LA also was co-localized with ZO-1 (Alexa Fluor 594) in separate tissue sections. In addition, von Willebrand Factor (vWF) IHC was used as a measure of vessel number.

### FITC-LA leakage

The leakage of FITC-LA (MW= 69-70 kDa, Sigma, St. Louis, MO) from the vasculature into the brain parenchyma was assessed as described previously (Carvey et al., 2005) to determine BBB integrity. In brief, 4 days following the last MPTP or saline injections, the mice were anesthetized with pentobarbital (60 mg/kg). 100 μl heparin (100 units/kg in Hank's Balanced Salt Solution; Life technologies) was injected intracardially followed immediately by 5 ml FITC-LA (5 mg/ml in 0.1M PBS) injected at a rate of 1.5 ml/min with the right atrium open ensuring a complete perfusion circuit. The perfusion pressure used to deliver FITC-LA was more than adequate to fill the brain's vascular compartment and similar to mouse blood pressure (unpublished observation). After perfusion, the brains were removed immediately and immersed into 4% paraformaldehyde and stored at 4°C. Twenty-four hours later, the fixative was replaced with three 24-h changes of 30% sucrose in 0.1 M PBS buffer. Each brain was sectioned at 40 μm using a sliding microtome, divided into 6 consecutive free-floating series and stored in cryoprotectant (0.05 M PBS with 30% sucrose and 30% ethylene glycol).

### Immunohistochemistry (IHC)

For integrin β3 IHC, the sections from one series were stained overnight at 4°C with primary antibody (Purified Hamster Anti-mouse CD61, 1:50 dilution; BD Pharmingen), followed by biotinylated secondary antibody (goat vs. hamster IgG, 1:100 dilution; Vector laboratories). Biotinylated antibody complex was amplified using an avidin-biotin complex kit (ABC-Elite Kit; Vector laboratories) and visualized with 3,3′-diaminobenzidine (DAB; Vector laboratories). Selected sections were processed for vWF as a marker for blood vessels. vWF (rabbit anti-human von Willebrand factor polyclonal antibody, 1:100 dilution, Millipore) was incubated with the sections overnight. Immunolabeling was continued using biotinylated secondary antibody (goat vs. rabbit IgG, 1:200 dilution; Vector laboratories) and then processed using ABC and DAB as described above. Additional sections were also processed for Iba-1 as a marker for microglia, TH as a marker for DA cells and Nissl a marker for all cells. Iba-1 IHC used a primary antibody (goat polyclonal to Iba-1, 1:500 dilution; Abcam), secondary antibody (horse anti-goat IgG, 1:200 dilution; Vector laboratories) and was visualized using ABC and DAB. Sections from each animal were stained for TH (primary antibody: anti-tyrosine hydroxylase rabbit pAB, 1:1600 dilution; Calbiochem, secondary antibody: goat vs. rabbit IgG, 1:400 dilution; Vector laboratories) and enhanced using the DAB protocol. Slides stained with TH were subsequently stained for Nissl using cresyl violet. Sections were mounted on gelatin-coated slides, dehydrated, and cover-slipped for imaging.

### Immunofluorescence

Immunofluorescence sections underwent an antigen unmasking step (i.e., citric acid buffer incubation for 30 min, at 80°C water bath, Vector laboratories). Autofluorescence was quenched with 1mg/ml $NaBH_4$ in, PBS pH 7.4 (Ding et al., 1995; Eddy et al., 2002). For β3 detection, the sections from one series were stained overnight at 4°C with primary antibody (Purified Hamster Anti-mouse CD61, 1:50 dilution; BD Pharmingen), followed by incubation with Texas Red secondary antibody (goat vs. hamster IgG, 1:100 dilution, Vector laboratories). To visualize ZO-1, sections were incubated for 1-h with a ZO-1, mouse monoclonal antibody, 7.5 μg/ml that was labeled with Alexa Fluor 594. Imaging was performed using fluorescence microscopy (Olympus, Model: IMT-2, Japan)

### Stereological assessment of immunoreactivity (ir) of TH-ir, Iba1-ir, and Nissl cell counts

Stereological assessment of TH-ir and Nissl stained cells in midbrain sections was limited to the SNpc (defined as tissue lateral to the accessory optic tract and superior to the reticulata).

Iba1-ir cells were assessed stereologically throughout the SN. The estimation of the total number of TH-ir neurons and activated microglia was performed using the computerized optical disector method (MicroBrightField software) as previously described (Zhao et al., 2007). In brief, a 5 X objective lens was used to define the contour around the entire region of interest and a 100 X lens was used for TH-ir and Iba1-ir cell count assessments. TH-ir cells and Iba1-ir cells were counted using a 250μm by 250μm optical disector frame at 100 X. The total number of TH-ir or Iba1-ir cells from each animal was estimated using the serial section manager software. One series of each animal was analyzed for TH-ir and Iba1-ir. Slides used for TH-ir cell counts were also used to perform stereological assessment of Nissl cell counts in the SNpc. Similar parameters were employed to perform Nissl cell stereology.

### Stereological assessment of vWF positive vessels

We estimated the total number of vessels present in the SN by following the same parameters described in Barcia et al. (Barcia et al., 2005). Briefly, a 5X objective lens was used to define the contour around the entire SN area and a 10 X lens was used for vessel assessment. Vessels were counted using a 300μm by 300μm optical disector frame.

### Statistical analyses

All values were expressed as mean ± SEM. One way analysis of variance (ANOVA) was used to determine statistical significance. Where noted, the *Tukey-Kramer or the Dunnett post hoc* tests were used to determine differences between groups or control, respectively.

## Results

### cyRGDfV attenuated MPTP induced integrin β3 immunoreactivity

Sections from animals intoxicated with MPTP, with or without cyRGDfV treatment, were processed for integrin β3 IHC. According to published studies (Brooks et al., 1994a; Brooks et al., 1994b), integrin β3 is expressed only on vessels undergoing angiogenesis, but not on patent vessels. The virtual absence of β3 immunoreactivity in Sal/Sal treated mice was in sharp contrast to expression of β3 immunoreactivity in the SN of MPTP/Sal animals (Fig 1). Higher magnification revealed that β3 immunoreactivity was confined to vessels (Fig 1 inset). A similar pattern of integrin β3 staining was observed in MPTP mice that received the control peptide, cyRADfV, (Fig 1). In contrast, the angiogenic inhibitor, cyRGDfV, that targets αvβ3 completely blocked β3 staining in the SN of MPTP animals (Fig 1). These data suggest that treatment with MPTP induced β3 upregulation and that cyRGDfV treatment 24-h later prevented or reversed β3 expression.

### cyRGDfV attenuated MPTP induced BBB dysfunction

In previous studies we used leakage of FITC-LA as a marker for disruption of the BBB (Carvey et al., 2005; Zhao et al., 2007). In those studies, there was leakage in the SN, but the anatomical location of the leakage within the SN varied from animal to animal and was best described as punctate (Carvey et al., 2005; Zhao et al., 2007). Likewise, all animals showed a diffuse leakage in the circumventricular regions including the hypothalamus and area postrema; regions which lack a BBB barrier (Zhao et al., 2007). However, no leakage was detected in the parietal cortex or hippocampus indicating that DA neurotoxins specifically affected the nigrostriatal pathway (Carvey et al., 2005; Zhao et al., 2007). In addition, we previously showed that FITC-LA leakage co-localized with integrin β3, a marker for angiogenesis in the 6-OHDA model of PD (Carvey et al., 2005). Here we determined if FITC-LA leakage co-localized with β3 following MPTP treatment and if anti-angiogenic peptides affected both leakage and co-localization.

At sacrifice, ninety-six hours following MPTP treatment, FITC-LA was perfused into the common carotid artery. Areas of punctate FITC-LA leakage were evident in most sections of the SN from the MPTP/Sal treated animals as well as MPTP animals treated with the inactive control peptide, cyRADfV (Fig 2). The SN of both MPTP/Sal and MPTP/cyRADfV also exhibited increases in integrin β3. Note that the areas of BBB disruption, indicated by punctate areas of FITC-LA leakage, co-localized with integrin β3 (Fig 2, merged). As expected, no areas of FITC-LA leakage were found in the SN of Sal/Sal mice indicating an intact BBB and very low levels of β3 integrin were observed. However, cyRGDfV treatment markedly reduced β3 reactivity and FITC-LA leakage in MPTP treated mice, as no overt entry of FITC-LA into SN parenchyma was observed. These finding suggest that angiogenesis may be part of the mechanism responsible for MPTP-induced BBB dysfunction since the angiogenic inhibitor cyRGDfV reduced both β3 expression and BBB leakage.

### MPTP effects on vessel number

The initiation of angiogenesis by MPTP may increase vessel numbers. To assess this possibility, vessels were identified using vWF IHC and vWF positive vessels were counted using stereology as in Barcia et al. (Barcia et al., 2005). We observed significant increases in vessel numbers ($F_{(3,12)}$=13.735, $p<0.01$) and vessel numbers in the SN of MPTP/Sal ($p<0.01$) and MPTP/cyRADfV ($p<0.01$) mice were increased ~41% compared with Sal/Sal controls (Fig 3). However, we also found a similar increase in vascular number in the SN of the MPTP/cyRGDfV ($p<0.01$) group. Thus, anti-angiogenic treatment had no effect upon the increase in vessel number. It appears that MPTP initiated an initial angiogenic burst and that addition of the anti-angiogenic peptide on the following day was not sufficient to block vessel formation.

### cyRGDfV attenuated MPTP-induced loss of ZO-1 immunoreactivity

To further examine the effects of cyRGDfV on BBB dysfunction, ZO-1-ir was assessed. ZO-1 is a molecule integral to the formation of tight junctions of the BBB and thus critical for barrier integrity (Wolburg and Lippoldt, 2002). To verify antibody staining, ZO-1-ir was first examined in the hypothalamus and hippocampus. The medial hypothalamus lacks a BBB and examination of the circumventricular region of the hypothalamus revealed areas of reduced ZO-1-ir independent of treatment, contrasting with the normal pattern of ZO-1-ir observed more distal to the third ventricle (Fig 4; (Petrov et al., 1994). In contrast, the hippocampus revealed ZO-1 immunoreactivity that was evenly distributed, but confined to vessels (Fig 4) and was similarly unaffected by MPTP treatment (Fig 4). While it is difficult to get vessels that lie entirely within plane of a tissue section, and stain identically for two markers, it is clear that there is considerable overlap between the ZO-1 labeling and the FITC-LA filled vessels, and that in the hippocampus, there was no overt effect of MPTP treatment. These results suggest that the ZO-1-ir does not label areas lacking a BBB, but does label vessels that should possess a BBB, and these staining patterns occurred independent of MPTP treatment. ZO-1 can therefore be a useful tool in assessing BBB integrity.

We observed brighter and more uniform fluorescence of ZO-1 in the SN of Sal/Sal and MPTP/cyRGDfV treated mice than the MPTP/Sal and MPTP/cyRADfV animals (Fig 5). Note that the SN of MPTP/Sal and MPTP/cyRADfV treated animals appeared to have fewer resolved vessels with darker areas indicating less ZO-1-ir. It also should be noted that due to tissue thickness, it was not possible to resolve all vessels and that the fluorescent signal may have been comprised of both unresolved vessels and autofluorescence. Regardless, these data taken together, suggest that tight junctions are less evident in MPTP treated mice,

which serves to further reinforce the conclusion from the FITC-LA data that MPTP reduces BBB integrity and is prevented by cyRGDfV treatment.

Double immunofluorescence studies of FITC-LA and ZO-1 vessels in the SN revealed that ZO-1-ir was considerably brighter overall in the Sal/Sal and the MPTP/cyRGDfV treated mice (Fig 6). Moreover, in both of these groups FITC-LA and ZO-1 were highly co-localized (Fig 6 merged). In contrast ZO-1-ir was weaker overall in the MPTP/Sal and MPTP/cyRADfV animals where FITC-LA filled vessels appeared to be missing sections stained for ZO-1 (arrows Fig 6). Thus, post treatment with the angiogenic inhibitor, cyRGDfV, but not the control peptide cyRADfV, prevented the reduction of the tight junction protein ZO-1 following MPTP treatment.

## cyRGDfV reduced MPTP induced neuroinflammation

Iba1 immunohistochemistry was used as a marker of microglia (Iba1-ir is markedly up-regulated in activated microglia (Ito et al., 2001)). Stereological cell counts for Iba1-ir positive cells were significantly affected by treatment ($F_{(5,24)} = 11.008$; $p< 0.001$; Table 1). Sal/Sal animals exhibited lower numbers of Iba1-ir microglia in their SNs (Fig 7B), the vast majority of which had small, rounded cell bodies with delicate processes typical of resting microglia (Fig 7A). In contrast, MPTP treatment not only increased the numbers of Iba1-ir positive cells in both MPTP/Sal ($p < 0.05$) and MPTP/cyRADfV treated mice by approximately 80% ($p < 0.05$; Fig 7B), but also induced dramatic changes in their morphology (Fig 7A). Thus, the vast majority of the microglia in these animals had large cell bodies with highly ramified, thick processes typical of activated microglia (Fig 7A). In contrast, the stereological Iba1-ir cell counts revealed that cyRGDfV post-treatment significantly attenuated the overall increase in microglia ($p<0.05$ relative to MPTP/Sal). Moreover, the phenotypic morphology of these cells was, in most cases, similar to that in the Sal/Sal treated animals, although it was clear that some of the cells were also exhibiting signs of activation. cyRGDfV, when administered on its own, neither affected the Iba1-ir cell counts nor their phenotypes. These data suggest that post-treatment with the angiogenesis inhibitor cyRGDfV markedly attenuated the increase in numbers of microglia as well as morphological changes produced by MPTP.

## cyRGDfV attenuated MPTP-induced TH-ir cell losses

We assessed TH-ir cell counts in the SN stereologically as an index of DA neurons, since tyrosine hydroxylase is the rate-limiting enzyme in the synthesis of DA (Fernstrom and Fernstrom, 2007). The TH-ir cell counts in the mouse SN were typical of those reported previously (~11,300). However, the effects of the various treatments significantly affected those counts (Fig 8; $F_{(5,24)} = 16.890$; $p < 0.001$). Post-hoc comparisons of treatments using the Tukey-Kramer tests indicated that MPTP/Sal treated animals exhibited a significant 32% loss of TH-ir cells relative to Sal/Sal animals ($p < 0.001$). Similar losses were evident in the MPTP/cyRADfV group. In contrast, animals treated with MPTP/cyRGDfV and Sal/cyRGDfV exhibited no reductions in TH-ir cells. These data suggest that treatment with the angiogenic inhibitor cyRGDfV completely prevented the MPTP-induced reductions in TH-ir cell counts.

We also assessed Nissl counts to determine if the loss of TH-ir was a consequence of actual cell loss, or merely down-regulation of tyrosine hydroxylase (i.e., phenotypic suppression). If phenotype is suppressed by treatment, then apparent loss of TH-ir cells will be associated with increases in numbers of Nissl cells, whereas actual neuron loss will reveal reduced TH-ir cell counts with no changes in Nissl. Nissl cell counts in mice treated with MPTP or cyRGDfV were not significantly different from counts in the SNpc of the Sal/Sal treated mice ($44{,}044 \pm 2294$; $F_{(4,20)}=0.359$; $p=0.835$) although mice treated with MPTP/Sal

exhibited a non-significant decrease of 8%, which is similar to Nissl reductions following MPTP reported previously (Turmel et al., 2001). However, Nissl cell counts did not increase suggesting that the TH-ir cell loss observed was a consequence of actual cell loss.

## Discussion

The results from this study demonstrated that MPTP increased expression of the angiogenic marker β3 and vessel numbers in the SN in association with BBB leakage and down-regulation of the tight junction protein ZO-1. In addition, β3 integrin upregulation was co-localized with FITC-LA leakage suggesting that angiogenesis contributed, at least in part, to BBB compromise. These changes were also associated with increased numbers of Iba1-ir cells, microglial activation, and loss of TH-ir cells. In contrast, the anti-angiogenic peptide, cyRGDfV, which targets αvβ3, reduced β3 expression, prevented FITC-LA leakage and down-regulation of ZO-1 while preventing the increases in Iba1-ir cell counts and decreases in TH-ir normally produced by MPTP. However, cyRGDfV did not affect the MPTP-induced increases in vessel numbers. Taken together, these data suggest that angiogenesis occurs following MPTP exposure and administering cyRGDfV may possess neuroprotective benefits, ostensibly through its anti-angiogenic effect.

Several neurodegenerative diseases including stroke, amyotrophic lateral sclerosis, multiple sclerosis, Alzheimer's disease, and neuro-AIDS (Desai et al., 2009; Holley et al., 2010; Kirk et al., 2004; Pogue and Lukiw, 2004; Roscoe et al., 2009; Schultheiss et al., 2006; Thirumangalakudi et al., 2006; Vagnucci and Li, 2003; Zand et al., 2005) exhibit neuroinflammation and angiogenesis, and it would be therefore surprising if angiogenesis did not occur in PD or its animal models as suggested here. The data presented here strongly suggest that at least acutely, MPTP treated mice exhibited angiogenesis in the SN as evidenced by marked up-regulated expression of β3 integrin (Figs 1 and 2). Integrins exist as heterodimers and mediate attachment to the extracellular matrix. We used an antibody to the β3 subunit to probe for the presence of αvβ3 heterodimers on endothelial cells. αvβ3 is absent on patent vessels, but is expressed on angiogenic vessels where it facilitates endothelial cell division and migration. It has been widely used as a marker of angiogenesis (Brooks, 1996; Brooks et al., 1994a; Brooks et al., 1994b; Friedlander et al., 1995). The β3 subunit is not expressed in normal brain (Akiyama et al., 1991; Pinkstaff et al., 1999) and reports of its presence on cultured oligodendrocytes (Horton, 1990; Milner et al., 1997) is more likely a consequence of culturing since αvβ3 expression was not observed on the day of oligodendrocyte isolation. This suggests that increased β3 expression is indicative of angiogenesis in brain. However, the absence of β3 in normal brain rules out the expression of the αvβ3 heterodimer on brain tissue, but does not rule out the expression of other heterodimers containing αv. αv is expressed in brain in conjunction with β5 (Milner and Campbell, 2003) making the use of antibodies directed against αv or non specific antibodies against the vitronectin receptor(s) too non specific for angiogenesis. However, β3 antibodies will not cross react with αvβ5 and we and others have used a β3 integrin antibody to identify brain angiogenesis in animal models (Carvey et al., 2005; Schultheiss et al., 2006). It is therefore reasonable to assume that β3 expression is likely indicative of αvβ3 heterodimer up-regulation in brain indicating angiogenesis. Although using up-regulation of β3 solely on its own could be subject to debate, other findings in the present study implicate the involvement of angiogenesis in response to MPTP.

We and others have demonstrated that several DA neurotoxins lead to BBB dysfunction that can be associated with overt BBB compromise (i.e. leakage; (Carvey et al., 2005; Chen et al., 2008; Chung et al., 2010b; Zhao et al., 2007)). Punctate areas of MPTP-induced FITC-LA leakage in the SN were associated with overt up-regulation of β3 immunoreactivity in most cases (Fig 2). Thus, β3 up-regulation was often observed in the center of areas of

FITC-LA suggesting that maturing angiogenic vessels, which are inherently leaky (Baluk et al., 2004; Jain, 2003), may be the cause for leakage of this large protein into brain parenchyma. This does not rule out the possibility that FITC-LA leakage may be caused by non-angiogenic mechanisms, but does argue that angiogenesis can compromise barrier integrity. In addition, β3 up-regulation appeared to stain vessels (Fig 1 insert) as would be expected of an angiogenic marker. Also consistent with the notion that MPTP produces angiogenesis were the marked increases in the number of vWF profiles in the SN (Fig 3). Although the time from MPTP exposure to sacrifice was only 4 days, previous studies demonstrated that new vessels can form within 24 hours (Baluk et al., 2004; Chavakis et al., 2002). We also observed MPTP-induced reductions in expression of ZO-1 (Fig 5), a marker for tight junctions needed for BBB integrity (Kniesel and Wolburg, 2000). Maturing vessels do not exhibit intact tight junctions and angiogenic changes in brain were associated with reductions in ZO-1 in diabetic animals (Li et al., 2010). Moreover, high magnification photomicrographs of FITC-LA stained vessels exhibited reductions in ZO-1 consistent with angiogenic changes (Fig 6). Finally, previous studies reported angiogenic changes in animal models of PD (Barcia et al., 2005; Faucheux et al., 1999). Although it is clear that additional studies are needed to verify the presence of angiogenesis in toxin induced models of PD, the studies presented here strongly suggest its likelihood. Whether or not the TH-ir cell loss and increase in Iba1-ir cells indicative of DA neuron loss and neuroinflammation, respectively, following MPTP were merely associated with or a consequence of this angiogenesis requires further study. However, the results from the MPTP/cyRGDfV treated mice suggest that angiogenesis does participate in the effects of MPTP, and that preventing angiogenesis may be neuroprotective.

Administering cyRGDfV, a molecule similar to Cilengitide (Kawaguchi et al., 2001) that is currently in clinical trials as an anti-angiogenic, one day following MPTP treatment produced a dramatic attenuation of TH-ir cell loss (Fig 8). This suggests that preventing angiogenesis with cyRGDfV prevented DA neuron loss. However, it is possible that cyRGDfV simply interfered with the ability of MPTP to enter brain or alternatively, prevented the active metabolite of MPTP, 1-methyl-4-phenylpyridinium (MPP+), from entering DA neurons. However, studies using $^{3}$H-MPTP indicated that it entered the brain and was converted in astrocytes to MPP+ within minutes and that this metabolite was taken up by dopaminergic cells where it accumulated over a period of hours (Lyden et al., 1985; Speciale et al., 1998). Another study indicated that MPTP is cleared from the brain, necessitating hourly injections (Nwanze et al., 1995) while another study demonstrated that MPTP and MPP+ were almost completely cleared from the brain within 24 hours (i.e., 10% of initial levels remaining; (Zhang et al., 2008). Since we injected animals with cyRGDfV on the day after the first MPTP injection, it is highly unlikely that cyRGDfV directly interfered with MPTP or its metabolite. Moreover, cyRADfV, which is structurally very similar to cyRGDfV, did not prevent the MPTP-induced TH-ir cell loss similarly suggesting that structural interference with MPTP or MPP+ was not responsible for the prevention effect. However, it is also possible that cyRGDfV treatment interfered with expression of TH since this was used as a marker for DA neurons. This seems unlikely since Sal/cyRGDfV exhibited normal numbers of TH-ir cells (Table 1 and Fig 8). Likewise, MPTP treatment may have reduced expression of TH without killing DA neurons, since TH was used as a marker for DA neurons (i.e., so-called phenotypic suppression; (Bowenkamp et al., 1996), and cyRGDfV simply enhanced TH expression. We therefore performed Nissl staining in the SNpc in the same sections used for the TH-ir cell counting to determine if actual TH-ir cell loss was occurring. Overall, there were no statistically significant changes in the number of Nissl stained cells (Table I, Fig. 8). A non-significant decrease of 8% in the number of Nissl stained cells was observed in the MPTP/Sal group similar to the 9% loss of Nissl stained cells in a previous study (Turmel et al., 2001); but, Nissl stained cells did not increase. Thus, if TH had been simply suppressed in dopaminergic cells by treatment, they

would have stained for Nissl and the Nissl cell counts would have increased. Since this did not occur, it is very likely that cyRGDfV actually prevented the loss of DA neurons normally produced by MPTP. Taken together, these data strongly suggest that the complete attenuation of TH-ir cell loss produced by cyRGDfV in MPTP treated animals was a consequence of its binding to αvβ3.

Consistent with a role for αvβ3 in the observed effects, treatment with cyRGDfV, but not cyRADfV, prevented the up-regulation of β3 integrin in MPTP treated mice (Fig 1). Similarly, cyRGDfV, but not cyRADfV, also prevented the MPTP-induced FITC-LA leakage into brain parenchyma (Fig. 2). Both of these findings suggest that cyRGDfV prevented angiogenesis by binding to αvβ3 and stabilizing the BBB. Unfortunately, cyRGDfV also targets another αv containing integrin, αvβ5 (Friedlander et al., 1995). Like integrin αvβ3, expression of integrin αvβ5 is also dramatically increased on the endothelial surface during angiogenesis. Thus, cyRGDfV's anti-angiogenic effects may be the result of blocking either αvβ5 and/or αvβ3 mediated attachments. Blocking either integrin receptor is therefore still consistent with a role for angiogenesis in DA neuron loss. However, cyRGDfV may also have a direct effect on microglia, as microglia also express αvβ5 along with a host of other integrin receptors (Milner, 2009). Indeed, cyRGDfV prevented increases in Iba1-ir cells and largely attenuated the activation of microglia (Table I and Fig 7) suggesting that the effects observed here could have been a consequence of preventing the microglial activation that normally accompanies MPTP treatment. Indeed, we and others have shown that preventing microglial activation can prevent DA neuron loss following neurotoxin exposure (Chung et al., 2010a; Zhao et al., 2007) and a direct effect of cyRGDfV on microglia therefore cannot be ruled out.

Close examination of the microglia in the MPTP/cyRGDfV treated mice (Fig 7) revealed that some of the cells exhibited phenotypic changes indicative of activation (i.e., larger cell bodies with thicker processes) although most were similar to the thin, highly branched, small cell body microglia characteristic of quiescent cells (Kreutzberg, 1996). If cyRGDfV directly blocked αvβ5 receptors on microglia and reduced their activation, then neuroinflammatory cytokines including TNF-α and IL-1, which are also angiogenic (Sethi et al., 2008; Voronov et al., 2007), would have been reduced as well preventing the initiation of angiogenesis. However, this may not be the case given the vWF data.

It was clear that the numbers of vWF vessels were increased in MPTP/Sal and MPTP/cyRADfV treated mice indicating new vessel formation (Fig 3). However, MPTP/cyRGDfV mice exhibited similar increases in vWF. If cyRGDfV is anti-angiogenic, how could there be increases in vessel numbers? One possible explanation is that cyRGDfV was given too late after MPTP. Thus, cyRGDfV was given the day after MPTP and new vessel growth may have already been initiated, consistent with the findings of Baluk et al. and Chavakis et al. who demonstrated that initial vessel growth can be seen within one day of stimulation (Baluk et al., 2004; Chavakis et al., 2002). Thus, cyRGDfV did not stop the angiogenesis that was underway, but may have changed the characteristics of the vessels. This is consistent with the notion that anti-angiogenic treatments were initially devised to “starve the tumor,” but in practice they may be most effective in the normalization of the vasculature (Jain, 2005). While high doses may remove some immature vessels, anti-angiogenic treatment allows for the further development of immature vessels as evidenced by increased pericyte association and reduction in edema and interstitial pressure with better oxygenation (Tong et al., 2004; Winkler et al., 2004). In fact, an angiogenesis inhibitor was shown to restore the BBB in a mouse glioblastoma model (Claes et al., 2008) and in a middle cerebral artery occlusion model of stroke (Shimamura et al., 2006). It is quite possible that we did not have cyRGDfV onboard at an early enough time, or at a high enough dose to block the initial burst of angiogenic activity responsible for the increase in

vessel number. However, cyRGDfV likely dampened the angiogenic activity and allowed the vessels to mature stabilizing BBB function and reducing downstream inflammatory process. At this point, we do not have definitive data to determine if the neuroprotective effects of cyRGDfV on DA neurons is through an anti-angiogenic mechanism that stabilizes BBB function, indirectly affecting microglia, or if it is a direct effect of cyRGDfV on microglia activation. To rule out cyRGDfV's direct effect on microglia we plan to examine other angiogenic inhibitors in the future (e.g., anti-VEGF) to determine if the effects observed here are a class effect of anti-angiogenics or unique to cyRGDfV.

cyRGDfV also prevented the MPTP-induced reductions in ZO-1. Although FITC-LA has been widely used as an index of barrier integrity, it could be transported into brain (e.g., caveolae). If indeed MPTP was compromising barrier integrity and allowing entry of FITC-LA, then the tight junction protein ZO-1 would also be down-regulated or rearranged from its normal continuous pattern between endothelial cells (Beauchesne et al., 2009; Bennett et al., 2010; Chen et al., 2008). ZO-1was examined first in the circumventricular region of the hypothalamus, an area that lacks the BBB. In the circumventricular region of the hypothalamus, there was reduced ZO-1-ir (Fig 4) that corroborated our prior observations of diffuse FITC-LA leakage in this area (Zhao et al., 2007). In addition the halo of ZO-1-ir described by Petrov and colleagues (Petrov et al., 1994) was evident, reflecting no barrier adjacent to the third ventricle as expected with increasing ZO-1-ir away from the ventricle reflecting an intact barrier. In contrast, normal ZO-1-ir was observed in the hippocampus and was highly co-localized with FITC-LA filled vessels independent of treatment (Fig 4). The fact that MPTP treatment did not alter these patterns of immunoreactivity in either area suggests that ZO-1-ir is indeed indicative of BBB integrity.

In MPTP/Sal and MPTP/cyRADfV mice exhibiting FITC-LA leakage, ZO-1-ir was markedly reduced (Fig 5). The FITC-LA and ZO-1 co-localization images also indicated that the ZO-1-ir was discontinuous and sometimes missing from the MPTP/Sal and the MPTP/cyRADfV conditions suggesting down-regulation or reorganization (Fig 6). In taking these images, we chose not to focus on the obvious areas of FITC-LA leakage. Aside from the fact that the vessels were hard to define in leakage areas, the goal was to determine if there was a more wide-spread dysfunction of the BBB rather than an overt breach. This is particularly relevant since not all groups have observed overt barrier compromise in animal models of PD (Astradsson et al., 2009) and no human study has observed overt leakage in imaging studies. Thus, failure to observe leakage does not mean that the BBB is normal since neuroinflammation may induce alterations in tight junctions as well as alterations in expression of other endothelial cell proteins that are necessary for normal function. Regardless, cyRGDfV protected the down-regulation/reorganization of ZO-1 in MPTP treated animals (Figs 5 and 6) consistent with the hypothesis that it prevented angiogenesis, the associated effects on ZO-1 expression, and the barrier compromise in areas where the BBB was actually breached. These effects are consistent with an anti-angiogenic mechanism.

Unfortunately, the acute intoxication animal models of PD do not necessarily mimic the progressive nature of PD. If angiogenesis and its associated barrier dysfunction were to become chronic, it could contribute to disease progression. Prolonged neuroinflammation would be associated with continued production of pro-angiogenic factors including cytokines as well as VEGF which is increased in the SN and striatum of PD patients (Wada et al., 2006; Yasuda et al., 2007). The chronic effects of VEGF up-regulation have been studied in the context of tumor biology. Here prolonged exposure to VEGF can lead to pathological angiogenesis, where the vessels are continuously leaky, lack pericytes and raise interstitial pressure, preventing the efficient delivery of oxygen and nutrients (Nagy et al., 2008). Since hypoxia can drive the production of VEGF (Kenneth and Rocha, 2008), this

sets up a feed forward loop perpetuating the pathological angiogenesis. The resulting dysfunctional barrier could then allow entry of peripheral vascular elements including toxins and adaptive immune elements that have been shown to contribute to DA neuron loss (Brochard et al., 2009). If this were the case, the use of anti-angiogenic drugs that are already approved by the FDA (e.g., the anti-VEGF drug, Avastin) or in phase III clinical trials (e.g., Cilengitide) might be useful in slowing PD progression.

## Acknowledgments

This work was supported by a grant from the Kenneth Douglass Foundation and NINDS R01-N5052414.

## References

Akiyama H, Kawamata T, Dedhar S, McGeer PL. Immunohistochemical localization of vitronectin, its receptor and beta-3 integrin in Alzheimer brain tissue. J Neuroimmunol. 1991; 32:19–28. [PubMed: 1705945]

Antonini A, Moresco RM, Gobbo C, De Notaris R, Panzacchi A, Barone P, Bonifati V, Pezzoli G, Fazio F. Striatal dopaminergic denervation in early and late onset Parkinson's disease assessed by PET and the tracer [11C]FECIT: preliminary findings in one patient with autosomal recessive parkinsonism (Park2). Neurol Sci. 2002; 23 2:S51–52. [PubMed: 12548339]

Astradsson A, Jenkins BG, Choi JK, Hallett PJ, Levesque MA, McDowell JS, Brownell AL, Spealman RD, Isacson O. The blood-brain barrier is intact after levodopa-induced dyskinesias in parkinsonian primates--evidence from in vivo neuroimaging studies. Neurobiol Dis. 2009; 35:348–351. [PubMed: 19501164]

Aumailley M, Gurrath M, Muller G, Calvete J, Timpl R, Kessler H. Arg-Gly-Asp constrained within cyclic pentapeptides. Strong and selective inhibitors of cell adhesion to vitronectin and laminin fragment P1. FEBS Lett. 1991; 291:50–54. [PubMed: 1718779]

Baluk P, Lee CG, Link H, Ator E, Haskell A, Elias JA, McDonald DM. Regulated angiogenesis and vascular regression in mice overexpressing vascular endothelial growth factor in airways. Am J Pathol. 2004; 165:1071–1085. [PubMed: 15466375]

Barcia C, Bautista V, Sanchez-Bahillo A, Fernandez-Villalba E, Faucheux B, Poza y Poza M, Fernandez Barreiro A, Hirsch EC, Herrero MT. Changes in vascularization in substantia nigra pars compacta of monkeys rendered parkinsonian. J Neural Transm. 2005; 112:1237–1248. [PubMed: 15666038]

Barcia C, Emborg ME, Hirsch EC, Herrero MT. Blood vessels and parkinsonism. Front Biosci. 2004; 9:277–282. [PubMed: 14766365]

Beauchesne E, Desjardins P, Hazell AS, Butterworth RF. Altered expression of tight junction proteins and matrix metalloproteinases in thiamine-deficient mouse brain. Neurochem Int. 2009; 55:275–281. [PubMed: 19576514]

Bennett J, Basivireddy J, Kollar A, Biron KE, Reickmann P, Jefferies WA, McQuaid S. Blood-brain barrier disruption and enhanced vascular permeability in the multiple sclerosis model EAE. J Neuroimmunol. 2010; 229:180–191. [PubMed: 20832870]

Bowenkamp KE, David D, Lapchak PL, Henry MA, Granholm AC, Hoffer BJ, Mahalik TJ. 6-hydroxydopamine induces the loss of the dopaminergic phenotype in substantia nigra neurons of the rat. A possible mechanism for restoration of the nigrostriatal circuit mediated by glial cell line-derived neurotrophic factor. Exp Brain Res. 1996; 111:1–7. [PubMed: 8891630]

Brochard V, Combadiere B, Prigent A, Laouar Y, Perrin A, Beray-Berthat V, Bonduelle O, Alvarez-Fischer D, Callebert J, Launay JM, Duyckaerts C, Flavell RA, Hirsch EC, Hunot S. Infiltration of CD4+ lymphocytes into the brain contributes to neurodegeneration in a mouse model of Parkinson disease. J Clin Invest. 2009; 119:182–192. [PubMed: 19104149]

Brooks PC. Role of integrins in angiogenesis. Eur J Cancer. 1996; 32A:2423–2429. [PubMed: 9059330]

Brooks PC, Clark RA, Cheresh DA. Requirement of vascular integrin alpha v beta 3 for angiogenesis. Science. 1994a; 264:569–571. [PubMed: 7512751]

Brooks PC, Montgomery AM, Rosenfeld M, Reisfeld RA, Hu T, Klier G, Cheresh DA. Integrin alpha v beta 3 antagonists promote tumor regression by inducing apoptosis of angiogenic blood vessels. Cell. 1994b; 79:1157–1164. [PubMed: 7528107]

Brown LF, Detmar M, Claffey K, Nagy JA, Feng D, Dvorak AM, Dvorak HF. Vascular permeability factor/vascular endothelial growth factor: a multifunctional angiogenic cytokine. Exs. 1997; 79:233–269. [PubMed: 9002222]

Carvey PM, Hendey B, Monahan AJ. The blood-brain barrier in neurodegenerative disease: a rhetorical perspective. J Neurochem. 2009; 111:291–314. [PubMed: 19659460]

Carvey PM, Zhao CH, Hendey B, Lum H, Trachtenberg J, Desai BS, Snyder J, Zhu YG, Ling ZD. 6-Hydroxydopamine-induced alterations in blood-brain barrier permeability. Eur J Neurosci. 2005; 22:1158–1168. [PubMed: 16176358]

Caudle WM, Zhang J. Glutamate, excitotoxicity, and programmed cell death in Parkinson disease. Exp Neurol. 2009; 220:230–233. [PubMed: 19815009]

Chavakis E, Riecke B, Lin J, Linn T, Bretzel RG, Preissner KT, Brownlee M, Hammes HP. Kinetics of integrin expression in the mouse model of proliferative retinopathy and success of secondary intervention with cyclic RGD peptides. Diabetologia. 2002; 45:262–267. [PubMed: 11935158]

Chen X, Lan X, Roche I, Liu R, Geiger JD. Caffeine protects against MPTP-induced blood-brain barrier dysfunction in mouse striatum. J Neurochem. 2008; 107:1147–1157. [PubMed: 18808450]

Chung YC, Kim SR, Jin BK. Paroxetine prevents loss of nigrostriatal dopaminergic neurons by inhibiting brain inflammation and oxidative stress in an experimental model of Parkinson's disease. J Immunol. 2010a; 185:1230–1237. [PubMed: 20566832]

Chung YC, Ko HW, Bok E, Park ES, Huh SH, Nam JH, Jin BK. The role of neuroinflammation on the pathogenesis of Parkinson's disease. BMB Rep. 2010b; 43:225–232. [PubMed: 20423606]

Claes A, Wesseling P, Jeuken J, Maass C, Heerschap A, Leenders WP. Antiangiogenic compounds interfere with chemotherapy of brain tumors due to vessel normalization. Mol Cancer Ther. 2008; 7:71–78. [PubMed: 18187807]

Cuervo AM, Wong ES, Martinez-Vicente M. Protein degradation, aggregation, and misfolding. Mov Disord. 2010; 25 1:S49–54. [PubMed: 20187257]

Damier P, Hirsch EC, Agid Y, Graybiel AM. The substantia nigra of the human brain. II. Patterns of loss of dopamine-containing neurons in Parkinson's disease. Brain. 1999; 122(Pt 8):1437–1448. [PubMed: 10430830]

Desai BS, Schneider JA, Li JL, Carvey PM, Hendey B. Evidence of angiogenic vessels in Alzheimer's disease. J Neural Transm. 2009; 116:587–597. [PubMed: 19370387]

Ding M, Robinson JM, Behrens BC, Vandre DD. The microtubule cytoskeleton in human phagocytic leukocytes is a highly dynamic structure. Eur J Cell Biol. 1995; 66:234–245. [PubMed: 7774609]

Eddy RJ, Pierini LM, Maxfield FR. Microtubule asymmetry during neutrophil polarization and migration. Mol Biol Cell. 2002; 13:4470–4483. [PubMed: 12475966]

Fato R, Bergamini C, Leoni S, Strocchi P, Lenaz G. Generation of reactive oxygen species by mitochondrial complex I: implications in neurodegeneration. Neurochem Res. 2008; 33:2487–2501. [PubMed: 18535905]

Faucheux BA, Bonnet AM, Agid Y, Hirsch EC. Blood vessels change in the mesencephalon of patients with Parkinson's disease. Lancet. 1999; 353:981–982. [PubMed: 10459912]

Fernstrom JD, Fernstrom MH. Tyrosine, phenylalanine, and catecholamine synthesis and function in the brain. J Nutr. 2007; 137:1539S–1547S. discussion 1548S. [PubMed: 17513421]

Friedlander M, Brooks PC, Shaffer RW, Kincaid CM, Varner JA, Cheresh DA. Definition of two angiogenic pathways by distinct alpha v integrins. Science. 1995; 270:1500–1502. [PubMed: 7491498]

Ginsberg MH, Partridge A, Shattil SJ. Integrin regulation. Curr Opin Cell Biol. 2005; 17:509–516. [PubMed: 16099636]

Hindle JV. Ageing, neurodegeneration and Parkinson's disease. Age Ageing. 2010; 39:156–161. [PubMed: 20051606]

Holley JE, Newcombe J, Whatmore JL, Gutowski NJ. Increased blood vessel density and endothelial cell proliferation in multiple sclerosis cerebral white matter. Neurosci Lett. 2010; 470:65–70. [PubMed: 20036712]

Horton M. Vitronectin receptor: tissue specific expression or adaptation to culture? Int J Exp Pathol. 1990; 71:741–759. [PubMed: 1698447]

Hynes RO, Zhao Q. The evolution of cell adhesion. J Cell Biol. 2000; 150:F89–96. [PubMed: 10908592]

Ito D, Tanaka K, Suzuki S, Dembo T, Fukuuchi Y. Enhanced expression of Iba1, ionized calcium-binding adapter molecule 1, after transient focal cerebral ischemia in rat brain. Stroke. 2001; 32:1208–1215. [PubMed: 11340235]

Jain RK. Molecular regulation of vessel maturation. Nat Med. 2003; 9:685–693. [PubMed: 12778167]

Jain RK. Normalization of tumor vasculature: an emerging concept in antiangiogenic therapy. Science. 2005; 307:58–62. [PubMed: 15637262]

Kawaguchi M, Hosotani R, Ohishi S, Fujii N, Tulachan SS, Koizumi M, Toyoda E, Masui T, Nakajima S, Tsuji S, Ida J, Fujimoto K, Wada M, Doi R, Imamura M. A novel synthetic Arg-Gly-Asp-containing peptide cyclo(-RGDf==V-) is the potent inhibitor of angiogenesis. Biochem Biophys Res Commun. 2001; 288:711–717. [PubMed: 11676501]

Kenneth NS, Rocha S. Regulation of gene expression by hypoxia. Biochem J. 2008; 414:19–29. [PubMed: 18651837]

Kirk S, Frank JA, Karlik S. Angiogenesis in multiple sclerosis: is it good, bad or an epiphenomenon? J Neurol Sci. 2004; 217:125–130. [PubMed: 14706213]

Kniesel U, Wolburg H. Tight junctions of the blood-brain barrier. Cell Mol Neurobiol. 2000; 20:57–76. [PubMed: 10690502]

Kreutzberg GW. Microglia: a sensor for pathological events in the CNS. Trends Neurosci. 1996; 19:312–318. [PubMed: 8843599]

Lee JK, Tran T, Tansey MG. Neuroinflammation in Parkinson's disease. J Neuroimmune Pharmacol. 2009; 4:419–429. [PubMed: 19821032]

Li W, Prakash R, Kelly-Cobbs AI, Ogbi S, Kozak A, El-Remessy AB, Schreihofer DA, Fagan SC, Ergul A. Adaptive cerebral neovascularization in a model of type 2 diabetes: relevance to focal cerebral ischemia. Diabetes. 2010; 59:228–235. [PubMed: 19808897]

Lyden A, Bondesson U, Larsson BS, Lindquist NG, Olsson LI. Autoradiography of 1-methyl-4-phenyl-1,2,3,6-tetrahydropyridine (MPTP): uptake in the monoaminergic pathways and in melanin containing tissues. Acta Pharmacol Toxicol (Copenh). 1985; 57:130–135. [PubMed: 3877403]

Marti HH. Angiogenesis--a self-adapting principle in hypoxia. Exs. 2005:163–180. [PubMed: 15617478]

Maubant S, Saint-Dizier D, Boutillon M, Perron-Sierra F, Casara PJ, Hickman JA, Tucker GC, Van Obberghen-Schilling E. Blockade of alpha v beta3 and alpha v beta5 integrins by RGD mimetics induces anoikis and not integrin-mediated death in human endothelial cells. Blood. 2006; 108:3035–3044. [PubMed: 16835373]

Milner R. Microglial expression of alphavbeta3 and alphavbeta5 integrins is regulated by cytokines and the extracellular matrix: beta5 integrin null microglia show no defects in adhesion or MMP-9 expression on vitronectin. Glia. 2009; 57:714–723. [PubMed: 18985734]

Milner R, Campbell IL. The extracellular matrix and cytokines regulate microglial integrin expression and activation. J Immunol. 2003; 170:3850–3858. [PubMed: 12646653]

Milner R, Frost E, Nishimura S, Delcommenne M, Streuli C, Pytela R, Ffrench-Constant C. Expression of alpha vbeta3 and alpha vbeta8 integrins during oligodendrocyte precursor differentiation in the presence and absence of axons. Glia. 1997; 21:350–360. [PubMed: 9419010]

Nagy JA, Benjamin L, Zeng H, Dvorak AM, Dvorak HF. Vascular permeability, vascular hyperpermeability and angiogenesis. Angiogenesis. 2008; 11:109–119. [PubMed: 18293091]

Nwanze E, Souverbie F, Jonsson G, Sundstrom E. Regional biotransformation of MPTP in the CNS of rodents and its relation to neurotoxicity. Neurotoxicology. 1995; 16:469–477. [PubMed: 8584278]

Pearce RK, Owen A, Daniel S, Jenner P, Marsden CD. Alterations in the distribution of glutathione in the substantia nigra in Parkinson's disease. J Neural Transm. 1997; 104:661–677. [PubMed: 9444566]

Petrov T, Howarth AG, Krukoff TL, Stevenson BR. Distribution of the tight junction-associated protein ZO-1 in circumventricular organs of the CNS. Brain Res Mol Brain Res. 1994; 21:235–246. [PubMed: 8170348]

Pinkstaff JK, Detterich J, Lynch G, Gall C. Integrin subunit gene expression is regionally differentiated in adult brain. J Neurosci. 1999; 19:1541–1556. [PubMed: 10024342]

Pogue AI, Lukiw WJ. Angiogenic signaling in Alzheimer's disease. Neuroreport. 2004; 15:1507–1510. [PubMed: 15194884]

Przedborski S, Jackson-Lewis V, Naini AB, Jakowec M, Petzinger G, Miller R, Akram M. The parkinsonian toxin 1-methyl-4-phenyl-1,2,3,6-tetrahydropyridine (MPTP): a technical review of its utility and safety. J Neurochem. 2001; 76:1265–1274. [PubMed: 11238711]

Roscoe WA, Welsh ME, Carter DE, Karlik SJ. VEGF and angiogenesis in acute and chronic MOG((35-55)) peptide induced EAE. J Neuroimmunol. 2009; 209:6–15. [PubMed: 19233483]

Ruoslahti E, Pierschbacher MD. Arg-Gly-Asp: a versatile cell recognition signal. Cell. 1986; 44:517–518. [PubMed: 2418980]

Schultheiss C, Blechert B, Gaertner FC, Drecoll E, Mueller J, Weber GF, Drzezga A, Essler M. In vivo characterization of endothelial cell activation in a transgenic mouse model of Alzheimer's disease. Angiogenesis. 2006; 9:59–65. [PubMed: 16821113]

Sethi G, Sung B, Aggarwal BB. TNF: a master switch for inflammation to cancer. Front Biosci. 2008; 13:5094–5107. [PubMed: 18508572]

Shimamura N, Matchett G, Solaroglu I, Tsubokawa T, Ohkuma H, Zhang J. Inhibition of integrin alphavbeta3 reduces blood-brain barrier breakdown in focal ischemia in rats. J Neurosci Res. 2006; 84:1837–1847. [PubMed: 17016855]

Somanath PR, Malinin NL, Byzova TV. Cooperation between integrin alphavbeta3 and VEGFR2 in angiogenesis. Angiogenesis. 2009; 12:177–185. [PubMed: 19267251]

Speciale SG, Liang CL, Sonsalla PK, Edwards RH, German DC. The neurotoxin 1-methyl-4-phenylpyridinium is sequestered within neurons that contain the vesicular monoamine transporter. Neuroscience. 1998; 84:1177–1185. [PubMed: 9578404]

Szekanecz Z, Besenyei T, Paragh G, Koch AE. Angiogenesis in rheumatoid arthritis. Autoimmunity. 2009; 42:563–573. [PubMed: 19863375]

Thirumangalakudi L, Samany PG, Owoso A, Wiskar B, Grammas P. Angiogenic proteins are expressed by brain blood vessels in Alzheimer's disease. J Alzheimers Dis. 2006; 10:111–118. [PubMed: 16988487]

Tong RT, Boucher Y, Kozin SV, Winkler F, Hicklin DJ, Jain RK. Vascular normalization by vascular endothelial growth factor receptor 2 blockade induces a pressure gradient across the vasculature and improves drug penetration in tumors. Cancer Res. 2004; 64:3731–3736. [PubMed: 15172975]

Turmel H, Hartmann A, Parain K, Douhou A, Srinivasan A, Agid Y, Hirsch EC. Caspase-3 activation in 1-methyl-4-phenyl-1,2,3,6-tetrahydropyridine (MPTP)-treated mice. Mov Disord. 2001; 16:185–189. [PubMed: 11295768]

Vagnucci AH Jr, Li WW. Alzheimer's disease and angiogenesis. Lancet. 2003; 361:605–608. [PubMed: 12598159]

Voronov E, Carmi Y, Apte RN. Role of IL-1-mediated inflammation in tumor angiogenesis. Adv Exp Med Biol. 2007; 601:265–270. [PubMed: 17713014]

Wada K, Arai H, Takanashi M, Fukae J, Oizumi H, Yasuda T, Mizuno Y, Mochizuki H. Expression levels of vascular endothelial growth factor and its receptors in Parkinson's disease. Neuroreport. 2006; 17:705–709. [PubMed: 16641673]

Winkler F, Kozin SV, Tong RT, Chae SS, Booth MF, Garkavtsev I, Xu L, Hicklin DJ, Fukumura D, di Tomaso E, Munn LL, Jain RK. Kinetics of vascular normalization by VEGFR2 blockade governs brain tumor response to radiation: role of oxygenation, angiopoietin-1, and matrix metalloproteinases. Cancer Cell. 2004; 6:553–563. [PubMed: 15607960]

Wolburg H, Lippoldt A. Tight junctions of the blood-brain barrier: development, composition and regulation. Vascul Pharmacol. 2002; 38:323–337. [PubMed: 12529927]

Yasuda T, Fukuda-Tani M, Nihira T, Wada K, Hattori N, Mizuno Y, Mochizuki H. Correlation between levels of pigment epithelium-derived factor and vascular endothelial growth factor in the striatum of patients with Parkinson's disease. Exp Neurol. 2007; 206:308–317. [PubMed: 17604022]

Zand L, Ryu JK, McLarnon JG. Induction of angiogenesis in the beta-amyloid peptide-injected rat hippocampus. Neuroreport. 2005; 16:129–132. [PubMed: 15671861]

Zhang MY, Kagan N, Sung ML, Zaleska MM, Monaghan M. Sensitive and selective liquid chromatography/tandem mass spectrometry methods for quantitative analysis of 1-methyl-4-phenyl pyridinium (MPP+) in mouse striatal tissue. J Chromatogr B Analyt Technol Biomed Life Sci. 2008; 874:51–56.

Zhao C, Ling Z, Newman MB, Bhatia A, Carvey PM. TNF-alpha knockout and minocycline treatment attenuates blood-brain barrier leakage in MPTP-treated mice. Neurobiol Dis. 2007; 26:36–46. [PubMed: 17234424]

Zhu J, Chu CT. Mitochondrial dysfunction in Parkinson's disease. J Alzheimers Dis. 2010; 20 2:S325–334. [PubMed: 20442495]

Research highlights

> MPTP, an agent that induces dopamine neuron loss in a mouse model of PD also induces angiogenesis > an angiogenesis inhibitor, cyRGDfV, blocks the up regulation of the β3 integrin, a marker of angiogenesis > cyRGDfV also reduced BBB dysfunction by blocking MPTP effects on vessel leakage and tight junction protein ZO-1. > cyRGDfV also reduced MPTP effects on microglia activation and dopamine neuron loss

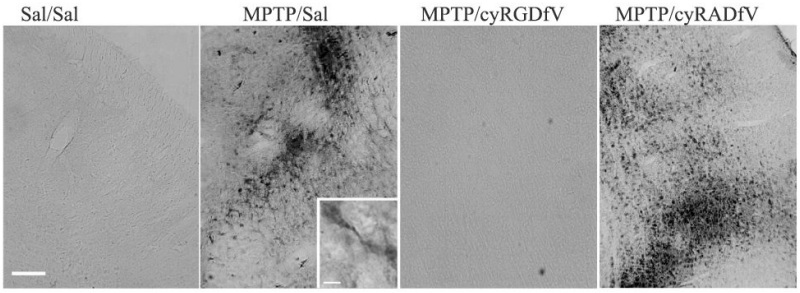


**Figure 1.**

Representative photomicrographs of β3 immunoreactivity in the substantia nigra of mice from the four treatment groups (scale bar = 100 μm). A representative higher magnification photomicrograph (scale bar = 20 μm) from an MPTP/Sal mouse reveals that the β3-ir was confined to vessels.

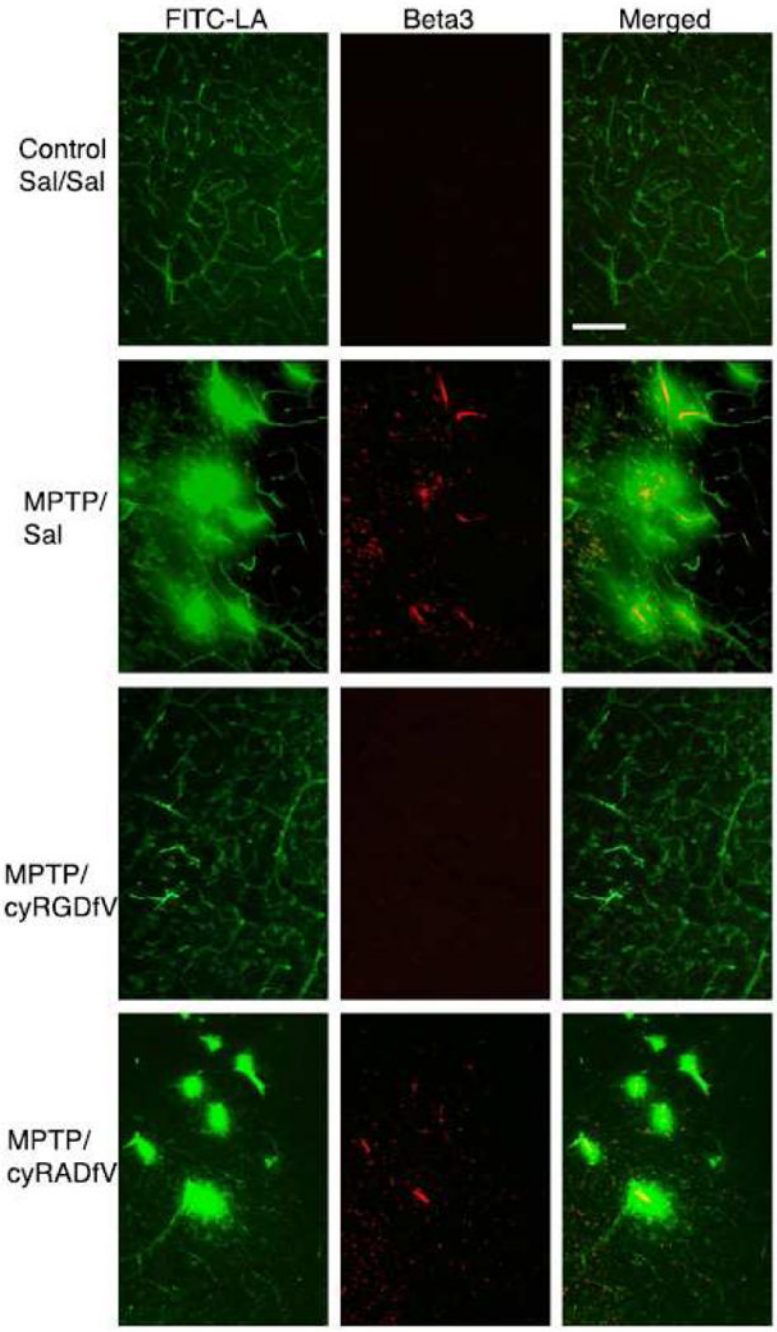


**Figure 2.**

Representative photomicrographs of FITC-LA (green) and β3-ir (red) in the substantia nigra from the four treatment groups. Note in the merged figures that the β3 is generally co-localized in the center of areas of FITC-LA leakage suggesting a relationship between β3 up-regulation and leakage. (scale bar = 100 μm)

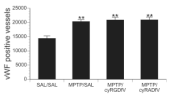


**Figure 3.**

Stereological counts of von Willebrand factor (vWF) immunoreactive vessels in the substantia nigra from the four treatment groups (n=4/group). (*Dunnett post hoc*; ** = $p<0.01$)

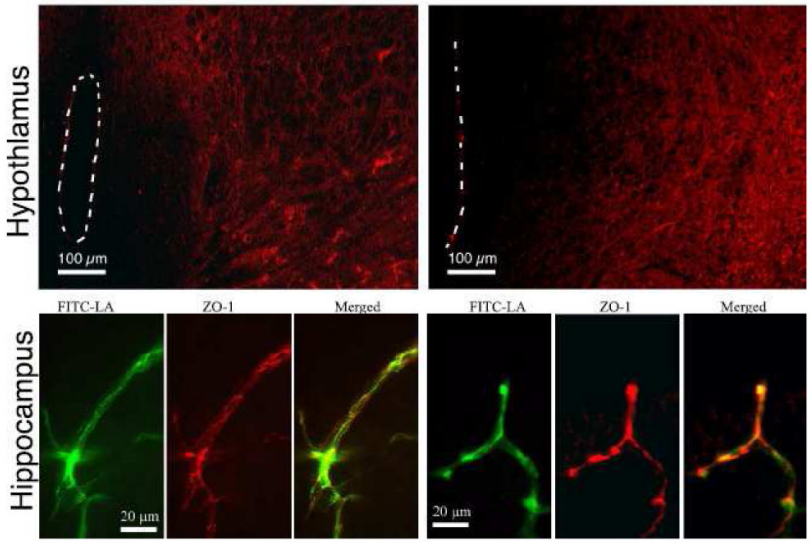


**Figure 4.**

Representative fluorescence photomicrographs of ZO-1 immunoreactivity in the hypothalamus and hippocampus of saline treated controls (left) and MPTP treated mice (right). The third ventricle is outlined. Note the characteristic halo effect around the ventricle where the BBB is absent (scale bar = 100 μm). In the hippocampus, note the extensive co-localization of ZO-1-ir on FITC-LA filled vessels (scale bar = 20 μm)

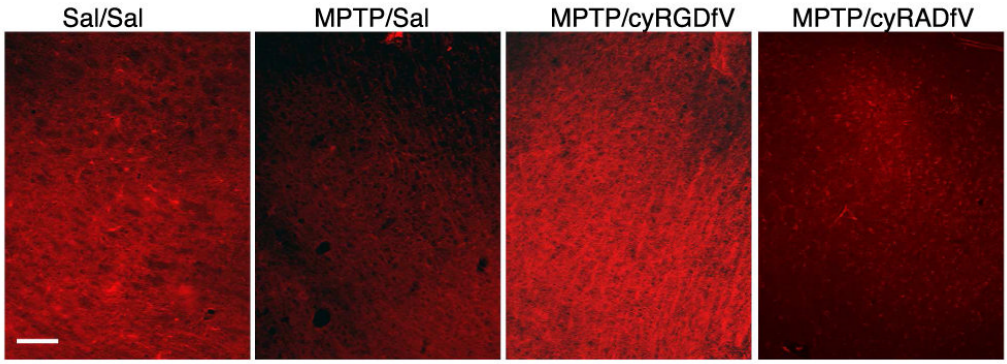


**Figure 5.**
Representative fluorescence photomicrographs of ZO-1 immunoreactivity in the SN of the four treatment groups. (scale bar is 100 μm)

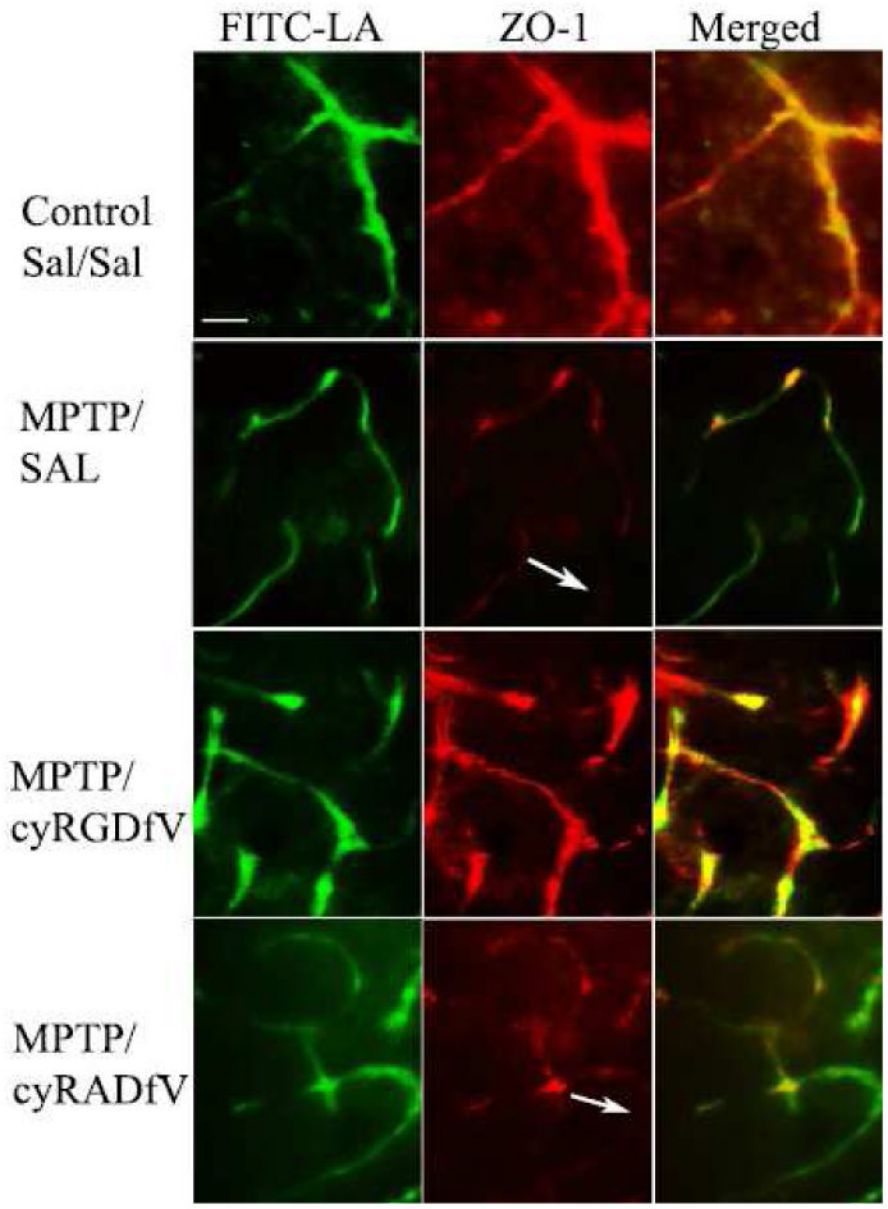


**Figure 6.**
Representative fluorescence photomicrographs of FITC-LA vessels (green) and ZO-1 immunoreactivity (red) in the SNpc of the four treatment groups. Note the reduction in ZO-1-ir co-localization in the MPTP/Sal and MPTP/cyRADfV merged images and apparent areas where there is no ZO-1-ir on a FITC-LA filled vessel (arrows). (scale bar = 20 μm)

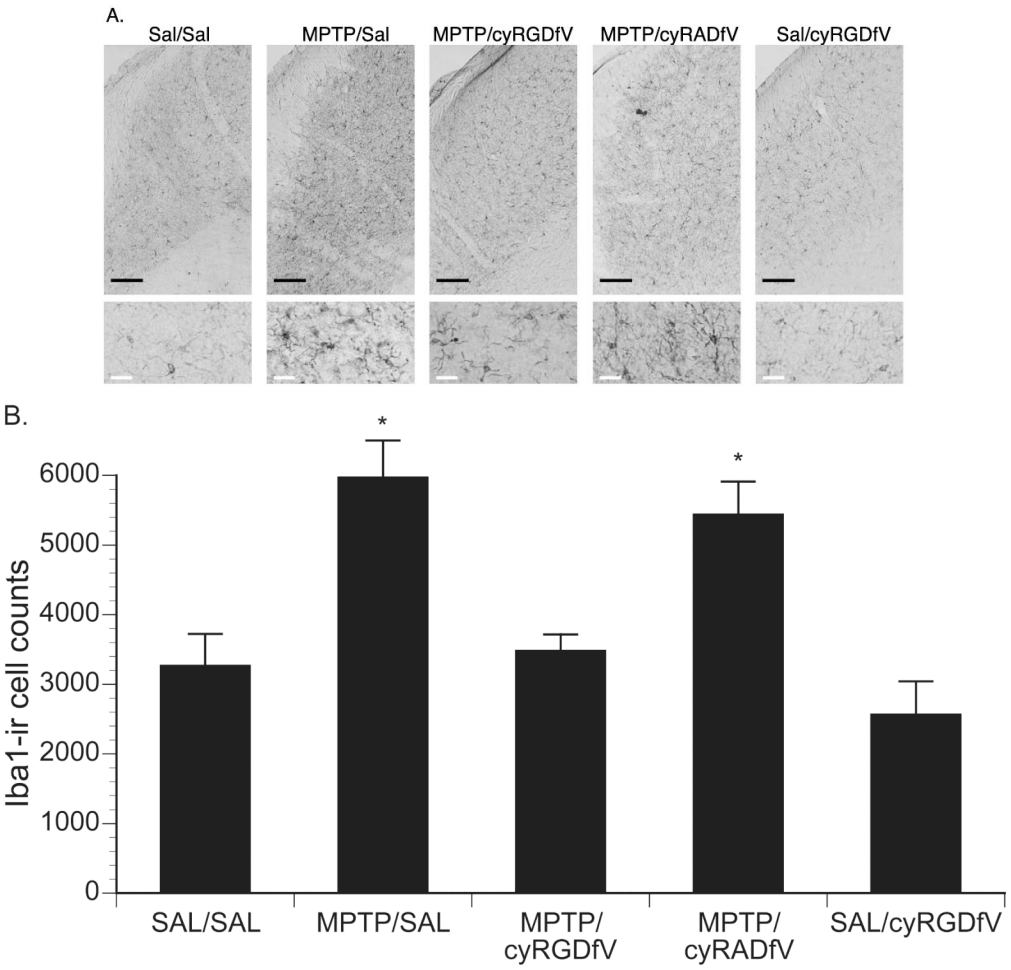


**Figure 7.**

(A) Representative low-power (top row; scale bar = 100 μm) and higher power (bottom row; scale bar = 20 μm) photomicrographs of Iba1-ir cells in the SN of the five treatment groups. Note the larger cell bodies and thicker process indicative of microglial activation in the MPTP/Sal and MPTP/cyRADfV groups compared with controls. (B) Stereological Iba1-ir cell counts from the SN of the five treatment groups (n=5/group). (*Tukey-Kramer post hoc* * = $p < 0.05$)

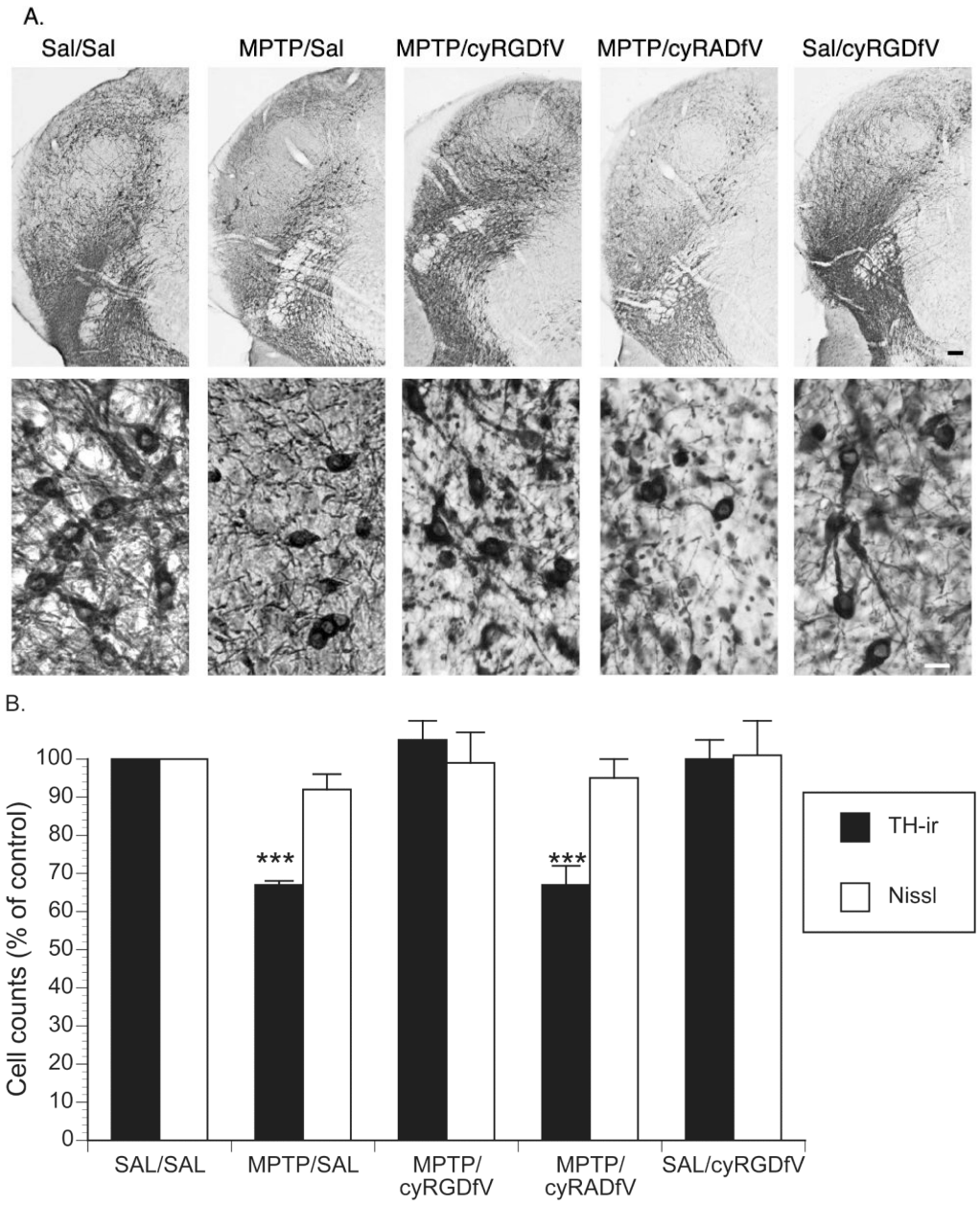


**Figure 8.**

(A) Representative low-power (top row; scale bar = 100μm) and higher power (bottom row; scale bar = 20 μm) photomicrographs of TH-ir cells in the substantia nigra of the five treatment groups. (B) Stereological TH-ir and Nissl cell counts expressed as their respective % of Sal/Sal treated means (± SEM) in the five treatment groups (n=5/group). (*Tukey-Kramer* post hoc *** = $p < 0.001$)

**Table 1**

**Cell Counts in SN† (mean ± SEM)**

| Treatment | Iba1-ir (microglia) | TH-ir (DA neurons) | Nissl (all cells) |
|---|---|---|---|
| **Sal/Sal** | 3265 ± 458 | 11279 ± 537 | 44044 ± 2294 |
| **MPTP/Sal** | *5972 ± 530 | ***7601±801 | 40377 ± 1847 |
| **MPTP/cyRGDfV** | 3483 ± 237 | 11834 ± 608 | 43495 ± 3392 |
| **MPTP/cyRADfV** | *5437 ± 475 | ***7535 ± 580 | 41881 ± 2050 |
| **Sal/cyRGDfV** | 2562 ± 479 | 11310 ± 605 | 44562 ± 4094 |

* = $p < 0.05$,

*** = $p < 0.001$, *Tukey-Kramer* post hoc

† TH-ir and Nissl counts were limited to the SNpc